IEEE Access
Multidisciplinary ⋮ Rapid Review ⋮ Open Access Journal

Received 6 December 2022, accepted 18 December 2022, date of publication 26 December 2022, date of current version 5 January 2023.

Digital Object Identifier 10.1109/ACCESS.2022.3232416

RESEARCH ARTICLE

Switching Investigation of SiC MOSFET Based 4-Quadrant Switch

NISHANT ANURAG, (Graduate Student Member, IEEE), AND SHABARI NATH, (Member, IEEE)
Department of Electronics and Electrical, IIT Guwahati, Guwahati, Assam 781039, India
Corresponding author: Nishant Anurag (anurag.nishant@iitg.ac.in)

This work was supported by the Science and Engineering Research Board, a Statutory Body of the Department of Science and Technology, Government of India.

ABSTRACT SiC MOSFETs are suited for several power electronic converters as they reduce loss, increase efficiency, withstand high temperatures and switch faster. SiC MOSFETs are 2-quadrant switches as they can block voltage of only one polarity. Many power converters require 4-quadrant switches, obtained by connecting two 2-quadrant switches. However, the present literature mostly examines the 2-quadrant operation of SiC MOSFETs apart from commercially unavailable monolithic 4-quadrant SiC MOSFETs. This paper, therefore, studies 4-quadrant switches based on SiC MOSFETs. It investigates in detail and finds the dominating devices for turn ON/OFF time and the trends of turn ON/ OFF time with respect to switch current for each quadrant. The paper further compares the maximum turn ON/OFF time of a 2-quadrant switch and a 4-quadrant switch. It also studies the effect of gate resistances on the turn ON/OFF time of the switch. The research is performed with the help of analysis, simulation, and experiment. The reasons behind the trends observed in the four quadrants are also analyzed. The paper finally summarizes the important observations about the turn ON/OFF time for SiC MOSFET based 4-quadrant switch.

INDEX TERMS 2-quadrant switch, 4-quadrant switch, matrix converter, SiC MOSFET, turn ON/OFF time.

I. INTRODUCTION

The switching characteristics of SiC MOSFETs suggest faster switching and lower switching loss [1]. The ON state characteristics suggest high current carrying capability, low conduction loss, and high junction temperature withstanding capability [2], [3], [4], [5]. Pertaining to the above advantageous features, SiC MOSFETs are best suited for power electronic converters as these reduce loss in converters and thus increase efficiency [6]. These also reduce filtering requirements for converters because the switching frequency increases compared to Si IGBTs at high voltage and current [7]. Further, for the same power rating, there is a reduction in the converter size [8]. Therefore, SiC MOSFETs are finding applications in high power density matrix converters [9], frequency converters in wind turbines [7], boost converters for fuel cell applications [6], and battery chargers in electric vehicles [8]. While SiC JFETs, IGBTs, and BJTs are also available, SiC MOSFETs are preferred due to advantages like normally-off operation, low turn-off loss due to lack of tail current, low on-state loss, and low gate charge [10], [11].

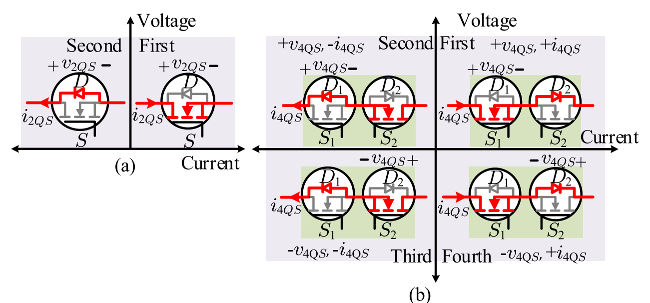

FIGURE 1. (a) Conducting and blocking device in MOSFET as a 2-quadrant switch. (b) Conducting and blocking devices in MOSFET based 4-quadrant switch.

A 4-quadrant switch blocks negative as well as positive voltage and also allows current in either direction [12]. Therefore, it is also called a bidirectional switch and is most suitable for converters dealing with alternating current and voltage. Hence, the applications of 4-quadrant switches are AC-AC

The associate editor coordinating the review of this manuscript and approving it for publication was Gian Domenico Licciardo.

This work is licensed under a Creative Commons Attribution-NonCommercial-NoDerivatives 4.0 License.
For more information, see https://creativecommons.org/licenses/by-nc-nd/4.0/

converters like matrix converters, cycloconverters, Vienna rectifiers, and single-stage solid-state transformers [13], [14]. Although Si-based [15], GaN-based [13], and SiC-based [16] monolithic 4-quadrant switches are present in the literature but are difficult to find commercially. Therefore, 4-quadrant switches are realisable using discrete 2-quadrant switches like Si IGBTs [17], SiC MOSFETs [14], [18], or SiC JFETs [19] and power diodes, if necessary. Given SiC MOSFETs have significant advantages over other devices, they are preferred for a 4-quadrant switch. The common-source configuration for the 4-quadrant switch is selected in this paper. The 4-quadrant switch based on reverse-blocking SiC MOSFETs shows more promising results than the common-source connection of conventional SiC MOSFETs [18], but these are commercially unavailable. Moreover, the common-source configuration has several benefits, which include independent control of current direction, reduced conduction losses, the applicability of body diodes of the MOSFETs, and the control of both MOSFETs from single isolated power supply [12].

Fig. 1(a) shows the conducting and blocking device of SiC MOSFET based 2-quadrant switch in first and second quadrants. In first quadrant, the current, i_{2QS}, flows through MOSFET S and the voltage, v_{2QS}, is blocked by it. In second quadrant, i_{2QS} flows through the body diode of S in the opposite direction and the polarity of voltage remaining the same is blocked by S. When two SiC MOSFETs are connected to form a 4-quadrant switch, several conditions arise which do not exist in the simple 2-quadrant operation of SiC MOSFET. The two SiC MOSFETs are subject to four different quadrants where both voltages and currents can be positive or negative. Further, the conducting and blocking devices of a particular quadrant are not the same. The conducting and blocking devices of SiC MOSFET based 4-quadrant switch in all four quadrants are shown in Fig. 1(b). In first quadrant MOSFET S_1 and body diode D_2 conduct the switch current, i_{4QS}, and the voltage, v_{4QS}, is blocked by MOSFET S_1. Whereas in second quadrant, MOSFET S_2 and body diode D_1 conduct due to reversal of i_{4QS} and v_{4QS} is blocked by MOSFET S_1. In third quadrant MOSFET S_2 and body diode D_1 conduct i_{4QS} and due to reversal of v_{4QS} the voltage is blocked by MOSFET S_2. Lastly, in fourth quadrant MOSFET S_1 and body diode D_2 conduct i_{4QS} and MOSFET S_2 blocks v_{4QS}. Also, the switching of a 4-quadrant switch involves the turn ON and turn OFF of two devices whereas there is only one device involved in the switching of 2-quadrant switch.

The existing literature mainly studies the 2-quadrant operation of SiC MOSFETs in detail. The authors in [1] have shown that increasing gate resistance of SiC MOSFET reduces the device voltage and current resonances and spikes, gate driver noise, cross talk, and EMI but lowers the switching speed and increases the switching loss. But they have not investigated the effect of gate resistances on the switching characteristics of SiC MOSFET based 4-quadrant switch. In common source configuration, [20] shows the switching characteristics of the 4-quadrant switch by performing a double pulse test. But characteristics under several operating conditions are missing. In [14], the forward and reverse conduction, switching characteristics of SiC MOSFET of the 4-quadrant switch, and voltage overshoot and oscillations due to parasitic inductances are shown. The authors in [21] also focus on the effect of common-source inductance on the voltage overshoot and oscillations of 4-quadrant switches, but none have analysed and shown the trends of turn ON and OFF times of the 4-quadrant switch. The turn ON/OFF times of the 4-quadrant switch are vital because these determine the maximum switching frequency of direct AC-AC matrix converters [22]. Although SiC MOSFETs have very low turn ON and OFF times when connected and operated as a 4-quadrant switch, then the turn ON and OFF times of the 4-quadrant switch may not match the speed of discrete SiC MOSFETs. Therefore, this paper presents the devices affecting the turn ON/OFF time of the 4-quadrant switch in each quadrant, trends of turn ON/OFF time in all four quadrants with respect to switch current, and the maximum turn ON/OFF time which shows that the switching frequency of the 4-quadrant switch reduces compared to 2-quadrant switch.

The objective of this paper is to study how the turn ON/OFF time gets affected due to the additional operating conditions when SiC MOSFETs are connected to form a 4-quadrant switch. Hence, in this study, SiC MOSFETs are not operated at the voltage and current limits specified in the datasheet. The voltages chosen are based on lab regulations on the limit of voltage and currents, capacity of equipment available in the lab, and margin kept for the safe operation of SiC MOSFETs. Hence the contributions of the paper are detailed.

1) The research provides a detailed study of switching of SiC MOSFET based 4-quadrant switch in all four quadrants, which are missing in the literature. It is performed with the help of analysis, simulations and experiments by developing a test circuit. The analysis is done with the approximate switching waveforms of the MOSFETs.
2) The analysis highlights the dominating devices of each quadrant, which determine the turn ON/OFF time of the 4-quadrant switch. The analysis is done on a 4-quadrant switch converter leg of a 2×1 matrix converter.
3) The research helps establish simulation and experimental trends of turn ON/OFF time with respect to switch current in all quadrants. The trends are helpful in finding out the maximum switching frequency while considering the load current for the 4-quadrant switch. The reasons for different trends are: (a) The turn ON/OFF time in first and third quadrants are decided by only one MOSFET of the switch. (b) The turn ON/OFF time in second and fourth quadrants also depend on the turn ON/OFF time of the MOSFET of the complementary switch.
4) The research also helps establish from experimental results that there is a reduction in switching frequency for the SiC MOSFET based 4-quadrant switch as

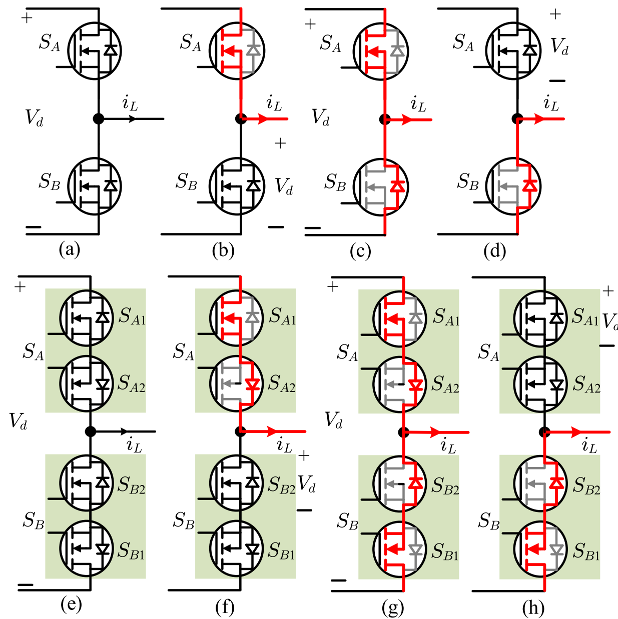

FIGURE 2. (a) A converter leg with 2-quadrant switch. (b) MOSFET S_A conducts the load current i_L before dead time. (c) Both S_A and the body diode of S_B conduct during dead time. (c) The body diode of S_B conducts after dead time. (e) A converter leg with 4-quadrant switches. (f) MOSFET S_{A1} and the body diode of S_{A2} carry the positive load current i_L. (g) S_{A1}, body diode of S_{A2}, S_{B1}, and body diode of S_{B2} conducts simultaneously during current commutation from S_A to S_B. (h) MOSFET S_{B1} and the body of S_{B2} carry the positive load current i_L.

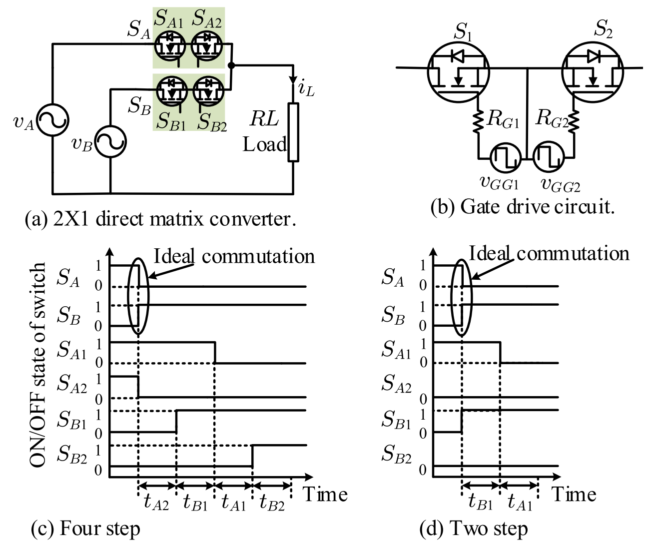

FIGURE 3. (a) A 2 × 1 direct matrix converter with 4-quadrant switches. (b) Gate drive circuit for a 4-quadrant switch. (c) Four step commutation. (d) Two step commutation.

compared to SiC MOSFET based 2-quadrant switch. This is deduced from the maximum turn ON/OFF time comparison of the switches in first and second quadrants.

5) This research also provides the experimental study of the effect of gate resistances on the turn ON/OFF time of the 4-quadrant switch. It shows that only the gate resistances of the dominating devices affect the turn ON/OFF time of the 4-quadrant switch. It is proved by using unequal gate resistances for the 4-quadrant switch.

This paper is organised as: Section II presents the characteristics of SiC MOSFET based 4-quadrant switch and factors affecting them. Section III describes the LTSpice simulation for turn ON/OFF of 4-quadrant switch. Section IV details the experimental verification, and Section V concludes the paper.

II. 2-QUADRANT VERSUS 4-QUADRANT SWITCH OPERATION

A 2-quadrant switch converter leg is shown in Fig. 2(a), with MOSFETs S_A and S_B. The voltage across the leg is V_d, and the load current is i_L. In this leg, the current conduction and the voltage blocking occur in one device. Fig. 2(b) shows that for positive i_L, S_A conducts if S_B blocks the voltage. In Fig. 2(d), the body diode of S_B conducts and S_A blocks the voltage. Similarly, for negative i_L, S_B conducts if S_A blocks the voltage and the body diode of S_A conducts if S_B blocks the voltage. This implies that the current flows through S_A, S_B, or the body diodes of the MOSFETs, and S_A or S_B blocks the voltage. Moreover, the current commutation from S_A to S_B involves dead time to avoid short circuit of the power supply. During the dead time, a part of i_L freewheels through the body diode of S_B because S_A starts turning OFF. The turn OFF time of S_A decides this dead time. The current commutation thus involves two devices- MOSFET and the body diode and the turn OFF of S_A is independent of S_B. When S_A turns ON, it dominates the turn ON process because the rate of fall of current in the body diode of S_B is decided by the rate of rise of current in S_A. Hence the turn ON/OFF time of S_A is independent of S_B.

In Fig. 2(e), a converter leg with 4-quadrant switches is shown. In this converter leg, the current conduction happens in two devices and voltage blocking by one device. For example, in the case of positive load current i_L, the current through the 4-quadrant switch S_A flows via S_{A1} and the body diode of S_{A2} and the voltage is blocked by S_{B1} in Fig. 2(f). Another example is shown in Fig. 2(h), where S_{B1} and the body diode of S_{B2} conduct and S_{A1} blocks the voltage. As a result, the current commutation involves four devices: S_{A1}, the body diode of S_{A2}, S_{B1}, and the body diode of S_{B2}, Fig. 2(g). Also, the 4-quadrant switch is subjected to operate in four quadrants. This forces the conducting and blocking devices to change according to the quadrant. Therefore, the analysis of the turn ON/OFF of 2-quadrant switch is not valid for turn ON/OFF of the 4-quadrant switch and requires separate analysis. The turn ON/OFF analysis of the 4-quadrant switch is, therefore presented in Section III.

III. TURN ON AND OFF OF SiC MOSFET BASED 4-QUADRANT SWITCH

The turn ON and OFF of SiC MOSFET based 4-quadrant switch are explained in this section with the help of a matrix converter. For a more straightforward explanation, the basic 2×1 matrix converter is chosen.

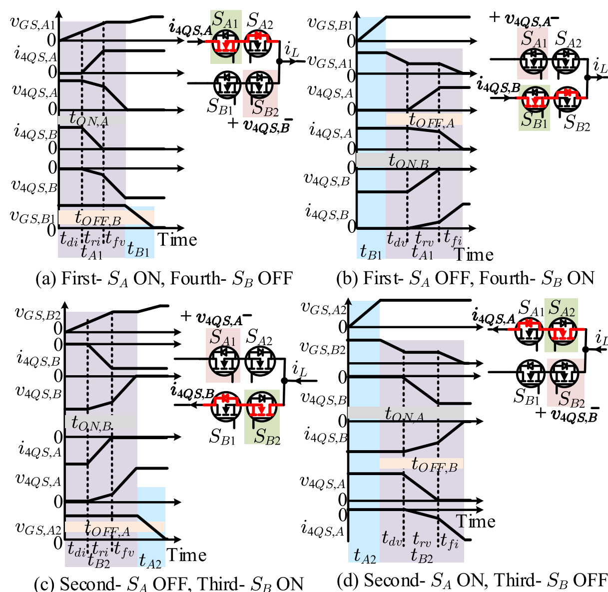

(a) First- S_A ON, Fourth- S_B OFF (b) First- S_A OFF, Fourth- S_B ON (c) Second- S_A OFF, Third- S_B ON (d) Second- S_A ON, Third- S_B OFF

FIGURE 4. Turn ON/OFF switching diagram of 4-quadrant switch.

A. DIRECT AC–AC MATRIX CONVERTER

The 2×1 matrix converter is shown in Fig. 3(a) with two 4-quadrant switches, S_A and S_B, connected to AC sources, v_a and v_b and current, i_L is through load RL. Further, there are two types of commutation processes for 4-quadrant switches in direct AC-AC converters - four step and two step [12]. In a conducting 4-quadrant switch, both MOSFETs are turned ON in four step commutation, as shown in Fig. 3(c), whereas only one MOSFET is turned ON in two step commutation, as presented in Fig. 3(d), assuming current commutates from S_A to S_B for positive current, i_L. The current commutation occurs in second or third step of four step commutation but current commutation occurs in first or second step of two step commutation. Therefore, the turn ON and OFF times of the 4-quadrant switch are decided in the above mentioned critical steps. The approximate switching waveforms during the critical steps are detailed further and the turn ON and OFF times of the 4-quadrant switch are established in all four quadrants.

B. TOTAL TURN ON/OFF TIMES IN FOUR QUADRANTS

When a SiC MOSFET is used as a 2-quadrant switch, the turn ON/OFF times are decided based on the turn ON/OFF of either the MOSFET or its body diode depending on the direction of the current and the gating of the MOSFET. However, the total turn ON and turn OFF times in a 4-quadrant switch are decided based on the turn ON/OFF of the conducting MOSFET, the series connected body diode, and the complementary 4-quadrant switch. In the literature, the total turn ON/OFF characteristics in different quadrants for the 4-quadrant switch based on SiC MOSFETs are missing and is studied in detail in this paper.

Fig. 4 presents the analysis of turn ON/OFF of the 4-quadrant switch in all the quadrants. In Fig. 4, the MOSFETs shaded in green and the series connected body diodes of the non-conducting MOSFETs conduct during the ON state. The current conduction path of the 4-quadrant switch is highlighted in red. The MOSFET, which blocks the voltage, is shaded in pink. The current in 4-quadrant switch S_A and S_B are $i_{4QS,A}$ and $i_{4QS,B}$, respectively. Similarly, the voltage across the switch S_A and S_B are $v_{4QS,A}$ and $v_{4QS,B}$, respectively. The turn ON/OFF of S_A and S_B are described below.

1) FIRST- S_A ON, FOURTH- S_B OFF

In Fig. 4(a),(b) the load current i_L is positive and hence $i_{4QS,A}$ and $i_{4QS,B}$ are also positive. For the analysis of turn ON/OFF, $v_A > v_B$ is assumed which makes $v_{4QS,A}$ positive and $v_{4QS,B}$ negative. Therefore, S_A operates in first quadrant, and S_B operates in fourth quadrant. Here, all the MOSFETs are considered identical. The Fig. 4(a) shows that S_{A1} and body diode of S_{A2} conduct $i_{4QS,A}$ in the ON state of S_A and body diode of S_{B2} blocks $v_{4QS,B}$ in the OFF state of S_B. The turn ON of S_A in first quadrant and turn OFF of S_B in fourth quadrant are shown in the switching diagram of Fig. 4(a). The gate-source voltage, $v_{GS,A1}$, of S_{A1}, is brought up, and the current $i_{4QS,A}$ starts rising after a current delay time, t_{di}, and attain its steady state after current rise time, t_{ri}. During this interval, $i_{4QS,B}$ starts falling and reaches zero. During voltage fall time, t_{fv}, $v_{4QS,A}$ and $v_{4QS,B}$ attain their steady states. The time taken for S_A to turn ON, $t_{ON,A} = t_{A1} = t_{di} + t_{ri} + t_{fv}$ and the current commutation occurs. After t_{A1} interval, the gate-source voltage of S_{B1}, $v_{GS,B1}$, goes down in time t_{B1} for complete turn OFF of S_B. There is an absence of voltage rise in S_{B1}, which eliminates the plateau voltage in $v_{GS,B1}$. Hence the time taken for S_B to turn OFF, $t_{OFF,B} = t_{ON,A} + t_{B1}$. From the analysis, it is evident that the turning ON of S_A involves S_{A1} only because the body diode of S_{A2} is always ON in first quadrant. Moreover, the turn OFF of S_B in fourth quadrant is dependent on the turn ON of S_A because of the favourable circuit condition for the conduction of S_A.

2) FIRST- S_A OFF, FOURTH- S_B ON

The blocking device for S_A is MOSFET S_{A1} in first quadrant, and the conducting devices for S_B are MOSFET S_{B1} and the body diode of S_{B2} in fourth quadrant, shown in Fig. 4(b). The switching waveforms are shown in Fig. 4(b). Here, $v_{GS,B1}$ goes high in time t_{B1}. There is an absence of plateau voltage in $v_{GS,B1}$ because there is no change in voltage across S_{B1}. Further, $v_{GS,A1}$ goes low and $v_{4QS,A}$ starts rising after voltage delay time, t_{dv}, and reaches its steady state in voltage rise time, t_{rv}. The current $i_{4QS,A}$ falls in current fall time, t_{fi}. Therefore, the time taken for S_A to turn OFF, $t_{OFF,A} = t_{A1} = t_{dv} + t_{rv} + t_{fi}$. During $t_{OFF,A}$, $v_{4QS,B}$ falls and $i_{4QS,B}$ rises to their respective steady states. Hence, the turn ON time for S_B, $t_{ON,B} = t_{B1} + t_{t_{OFF,A}}$. During the turn OFF of S_A, the body diode of S_{A2} does not turn OFF.

3) SECOND- S_A OFF, THIRD- S_B ON

The turn ON of S_B in third quadrant and turn OFF of S_A in second quadrant when i_L is negative is shown in Fig. 4(c).

The conducting devices of S_B are MOSFET S_{B1} and the body diode of S_B and the blocking device of S_A is MOSFET S_{A1}. The load current i_L is negative, and hence $i_{4QS,B}$ is also negative and $v_A > v_B$. The switching waveforms are shown in Fig. 4(c). Here, $v_{GS,B2}$ is brought up, and current $i_{4QS,B}$ starts rising in the negative direction after time t_{di} and reaches its steady state in t_{ri}. The complete fall of $v_{4QS,B}$ occurs in t_{fv} interval. Therefore, the time taken for S_B to turn ON, $t_{ON,B} = t_{B2} = t_{di} + t_{ri} + t_{fv}$. The current $i_{4QS,A}$ falls and the voltage $v_{4QS,A}$ rises in time t_{B2}. In the next step, $v_{GS,A2}$ goes down in t_{A2} time for complete turn OFF of S_A. The time taken for S_A to turn OFF, $t_{OFF,A} = t_{ON,B} + t_{A2}$. The actual switching of current and voltage occurs during $t_{ON,B}$ and turning ON of S_B involves S_{B2} only because the body diode of S_{B1} is always ON in third quadrant. The turn OFF of S_A in second quadrant is dependent on the turn ON of S_B because of the favourable circuit condition for conduction of S_B.

4) SECOND- S_A ON, THIRD- S_B OFF

Fig. 4(d) highlights that the MOSFET S_{A2} and the body diode of S_{A1} conducts in second quadrant of S_A. The blocking device for S_B in third quadrant is S_{B2}. Fig. 4(d) describes the switching waveforms of turn ON of S_A in the second quadrant and turn OFF of S_B in the third quadrant. Here, $v_{GS,A2}$ goes high in t_{A2} interval. In the next step, $v_{GS,B2}$ goes low in t_{B2}. During this interval, the voltage, $v_{4QS,B}$, starts rising after a delay time of t_{dv} and attains its steady state after a period of t_{rv}. The current, $i_{4QS,B}$, falls to zero in the interval t_{fi}. Further, there is simultaneous fall in voltage, $v_{4QS,A}$, during t_{rv} and rise in current, $i_{4QS,A}$, in the interval t_{fi}. The time taken for S_B to turn OFF, $t_{OFF,B} = t_{B2} = t_{dv} + t_{rv} + t_{fi}$. Also, the turn ON time for S_A, $t_{ON,A} = t_{A2} + t_{tOFF,B}$. The body diode of S_{B1} does not turn OFF.

When $v_A < v_B$, then S_A operates in third and fourth quadrants, and S_B operates in first and second quadrants according to the load current direction but switching characteristics remain similar to the characteristics explained above. Considering the operation of S_A in all four quadrants and from the above analysis, the quadrant-wise dominating devices of the converter leg for turn ON/OFF time of S_A is shown in Fig. 5. In first quadrant, S_{A1} decides the turn ON/OFF time of S_A, whereas S_{A2} decides the turn ON/OFF time in third quadrant. In second quadrant, S_{A2} and S_{B2} decide the the turn ON/OFF time of S_A and in fourth quadrant S_{A1} and S_{B1} decide the turn ON/OFF time.

C. EFFECT OF GATE RESISTANCE ON SWITCHING CHARACTERISTICS

The gate drive circuit for the 4-quadrant switch is shown in Fig. 3(b). The gate drive power supplies for S_1 and S_2 are v_{GG1} and v_{GG2}, respectively. The gate resistances for S_1 and S_2 are R_{G1} and R_{G2}, respectively. The choice of gate resistance values plays an important role in the turn ON/OFF of the 4-quadrant switch. The gate resistances of the same or different values can also be used for the two SiC MOSFETs of the switch, which verify the dominating devices for turn ON/OFF time. These effects, which are missing in the literature, are studied in detail.

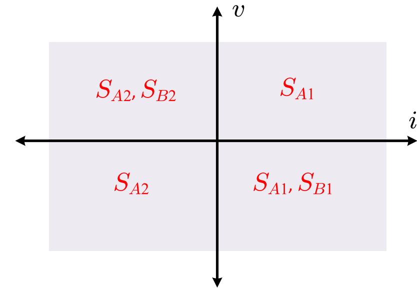

FIGURE 5. Quadrant wise dominating devices which determine the turn ON/OFF time of S_A.

From the above analysis of the turn ON/OFF time of the 4-quadrant switch considering switch S_A in first quadrant. The turn ON/OFF process of S_A depends on the turn ON/OFF of S_{A1} only. Therefore, only the gate resistance of S_{A1} affects the turn ON/OFF of S_A. Similarly, in third quadrant, the gate resistance of S_{A2} alone affects the turn ON/OFF time of S_A. In second quadrant, the gate resistance of the MOSFET S_{B2} affects the turn ON/OFF of S_B, which in turn affects the turn ON/OFF of S_A. Further, the gate resistance of S_{A2} also affects the rate of charging or discharging of the input capacitance of S_{A2}, which adds to the total turn ON/OFF time of S_A. In fourth quadrant, the gate resistances of S_{B1} and S_{A1} affect the turn ON/OFF time of S_A. Therefore, the gate resistance of S_{A1} affects the turn ON/OFF of S_A in first and fourth quadrants. Further, the gate resistance of S_{A2} affects the turn ON/OFF of S_A in second and third quadrants.

IV. LTspice SIMULATION FOR TURN ON/OFF OF 4-QUADRANT SWITCH

A. TURN ON/OFF TIME

The test circuit to obtain the switching characteristics of the 4-quadrant switch is shown in Fig. 6. The circuit has two SiC MOSFET based 4-quadrant switches connected in a half-bridge. The LTspice model of SiC MOSFET C2M0080120D is obtained from the manufacturer's website. V_{DC} is 120 V and two capacitors divide V_{DC} into two halves. The load R_o = 2 Ω and $L_o = 5\ mH$. Load current, $i_o = \hat{I}_o \sin \omega t + i_{sh}$, is obtained using sinusoidal pulse width modulation (PWM), where $\hat{I}_o = 20\ A$, $\omega = 100\,\pi\ rad/s$, i_{sh} is the current ripple at switching frequency, $f_s = 20\ kHz$. The load voltage v_o oscillates between $\frac{+V_{DC}}{2}$ and $\frac{-V_{DC}}{2}$. The simulation waveforms of i_o and v_o are shown in Fig. 7. The value of gate resistances R_{G1} and R_{G2} are 15 Ω. The gate drive power supplies v_{GG1} and v_{GG2} provide +20 V as positive gate drive voltage and −5 V as negative gate drive voltage for faster and reliable turn OFF of the MOSFET. Further, the model of HCPL-3120 gate driver IC is utilised to drive the SiC MOSFETs. Finally, the study of turn ON/OFF characteristics of the 4-quadrant switch is performed by operating S_A in first and second quadrants and S_B in third and fourth quadrants, as shown in Fig. 4.

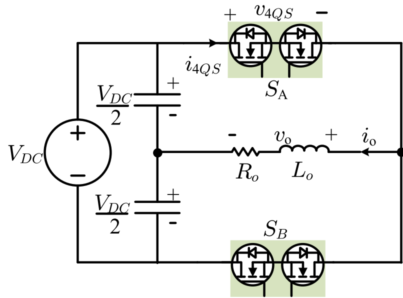

FIGURE 6. Test circuit for switching characteristics.

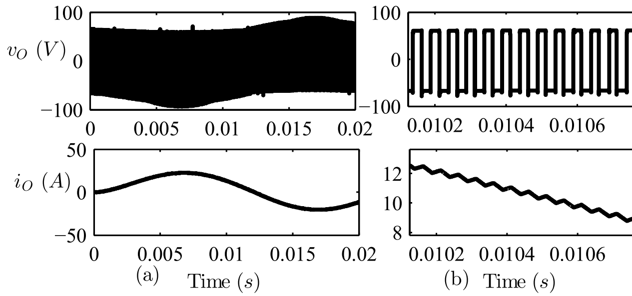

FIGURE 7. Simulated load voltage v_o and current i_o. (a) One cycle of load current i_o. (b) Magnified v_o and i_o at 20 kHz.

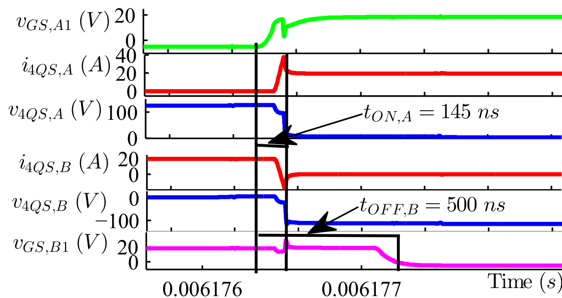

FIGURE 8. First: S_A turn ON. Fourth: S_B turn OFF.

1) S_A TURN ON IN FIRST AND S_B TURN OFF IN FOURTH

The LTspice simulation is shown in Fig. 8. The turn ON of S_A starts with the rise of voltage $v_{GS,A1}$ from -5 V. The current i_{4QSA} rises beyond the steady state value of $+20$ A because of the reverse recovery of the body diode of S_{B2}, which is visible in $i_{4QS,B}$ during the turn OFF of S_B. The voltage $v_{4QS,A}$ falls from $+120$ V to the ON state drop of $+6$ V. The turn ON time of S_A, $t_{ON,A}$, is 145 ns. The fall of current $i_{4QS,B}$ and the rise of voltage $v_{4QS,B}$ is in synchronism with $i_{4QS,A}$ and $v_{4QS,A}$, respectively. The voltage $v_{GS,B1}$ falls in the next step. The turn OFF time of S_B, $t_{OFF,B}$ is 500 ns. The intervals t_{A1}, t_{A2}, t_{B1}, and t_{B2} are kept equal to 250 ns in the control signal. Due to unequal propagation delays in the model of gate driver from low-high and high-low transitions, the intervals t_{A1}, t_{A2}, t_{B1}, and t_{B2} become unequal. Therefore, $t_{A1} > t_{B1}$ although the sum of t_{A1} and t_{B1} is 500 ns and that becomes a constant turn OFF time of S_B in fourth quadrant for any $i_{4QS,B}$.

2) S_A TURN OFF IN FIRST AND S_B TURN ON IN FOURTH

The simulation is shown in Fig. 9. The voltage $v_{GS,B1}$ rises to $+20$ V and in the next step $v_{GS,A1}$ falls to -5 V which makes the current $i_{4QS,A}$ to fall up to 0 A and the voltage $v_{4QS,A}$ rise till 120 V. Also, the voltage $v_{4QS,B}$ rises from -120 V to the ON state drop of $+6$ V. The current $i_{4QS,B}$ jumps to $+20$ A during this period. The turn OFF time for S_A, $t_{ON,A}$, is 78 ns and the turn ON time for S_B is 430 ns.

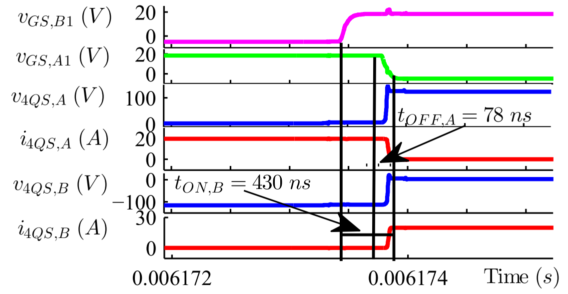

FIGURE 9. First: S_A turn OFF. Fourth: S_B turn ON.

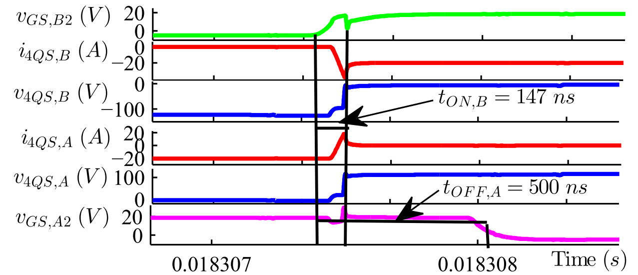

FIGURE 10. Second: S_A turn OFF. Third: S_B turn ON.

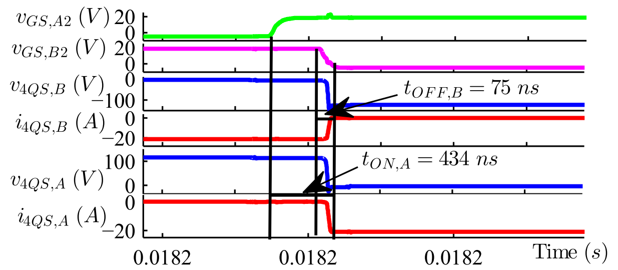

FIGURE 11. Second: S_A turn ON. Third: S_B turn OFF.

3) S_A TURN OFF IN SECOND AND S_B TURN ON IN THIRD

Fig. 10 presents the turn OFF of S_A in second quadrant and the turn ON of S_B in third quadrant. The turn ON of S_B in third quadrant is similar to the turn ON of S_A in first quadrant. Also, the turn OFF of S_A in second quadrant is similar to the turn OFF of S_B in fourth quadrant. Therefore, the turn ON time of S_B, $t_{ON,B}$, is 147 ns and the turn OFF time of S_A, $t_{OFF,A}$, is 500 ns. The currents $i_{4QS,A}$ and $i_{4QS,B}$ is -20 A during ON state and voltages $v_{4QS,A}$ and $v_{4QS,B}$ is $|120|$ V during OFF state.

4) S_A TURN ON IN SECOND AND S_B TURN OFF IN THIRD

The turn ON of S_A in second quadrant and the turn OFF of S_B in third quadrant is shown in Fig. 11. The turn OFF of S_B is similar to the turn OFF of S_A in first quadrant. This implies that the turn ON of S_A replicates the turn ON of S_B in fourth quadrant. The turn OFF time of S_B, $t_{OFF,B}$ is 75 ns and the turn ON time of S_A, $t_{ON,A}$, is 434 ns.

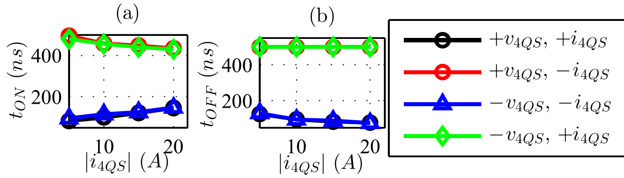

FIGURE 12. Simulation results showing (a) turn ON time t_{ON} and (b) turn OFF time t_{OFF} against $|i_{4QS}|$ of a 4-quadrant switch in all four quadrants.

Fig. 12(a) presents the turn ON time, t_{ON}, against current, i_{4QS}, of the 4-quadrant switch. In the first and third quadrants, t_{ON} is increasing in nature and lies well within 200 ns at 20 A. However, in the second and fourth quadrants, t_{ON} lies between 400-500 ns. The nature of the curve is decreasing, which attributes to the turn OFF time, t_{OFF}, curve of the complementary switch which operates in the first and third quadrants, shown in Fig. 12(b). The t_{OFF} curve monotonously decreases against increasing i_{4QS}. The voltage v_{4QS} is constant at $|120|$ V. The decline in t_{OFF} against increasing i_{4QS} is explained further with the help of the approximate turn OFF process of SiC MOSFET, shown in Fig. 13.

Fig. 13(a) is a simple test circuit for SiC MOSFET. A constant current, I_o, is assumed during the turn OFF of the MOSFET. The drain current i_D is constant at I_o before turn OFF, and V_{DC} provides the power supply. An ideal freewheeling diode FD is present to provide a path for I_o when the MOSFET turns OFF. Here, v_{GG} switches from V_{GG} to zero and the gate current, i_G, flows through the gate resistance, R_G, at the start of turn OFF. The parasitic capacitances of the MOSFET are shown, and other parasitics are neglected. Further, capacitance C_{GS} is assumed constant at 1035 pF taken from the datasheet of the SiC MOSFET throughout the turn OFF process. The capacitances C_{GD} and C_{DS} are the non-linear capacitances which vary with change in the drain-source voltage, v_{DS}. The voltage, $v_{DS} = V_{DS,ON}$, during the ON state. The gate-source voltage, v_{GS}, is at V_{GG} and gate-drain voltage, v_{GD}, is $V_{GG} - V_{DS,ON}$, before the turn OFF initiation. In this explanation, C_{GD} has three parts. A single value of $C_{GD} = 300$ pF is taken from the datasheet of the SiC MOSFET in the ON state. Then a range of non-linear values of C_{GD} is considered from the datasheet when v_{DS} varies in the active region from $V_{DS,ON}$ to V_{DC}. In the third part $C_{GD} = 15$ pF at $v_{DS} = V_{DC} = 120$ V. The effect of C_{DS} on the turn OFF process is neglected for keeping the explanation simple because its effect on the turn OFF process is negligible as compared to C_{GS} and C_{GD} [23]. In Fig. 13(b), at time, $t = t_o$, $v_{GS} = V_{GG}$; $v_{DS} = V_{DS,ON} \approx 0$; $i_D = I_o$; and $v_{GG} = 0$.

For $t_o < t \leq t_1$, $v_{DS} \approx 0$ and at $t = t_1$, v_{GS} is assumed constant at Miller voltage, V_{mil}, shown in Fig. 13(b) and $i_D = I_o \approx g_m(v_{GS} - V_{th})$ where, g_m is the transconductance of the MOSFET and V_{th} is the gate-source threshold voltage. Therefore, the $t_1 - t_0$ expression is deduced below.

$$i_G = -\frac{v_{GS}}{R_G} = C_{GS}\frac{dv_{GS}}{dt} + C_{GD}\frac{dv_{GD}}{dt} \quad (1)$$

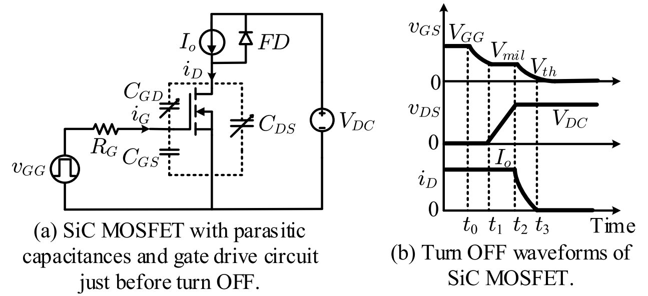

(a) SiC MOSFET with parasitic capacitances and gate drive circuit just before turn OFF.

(b) Turn OFF waveforms of SiC MOSFET.

FIGURE 13. Turn OFF process of SiC MOSFET.

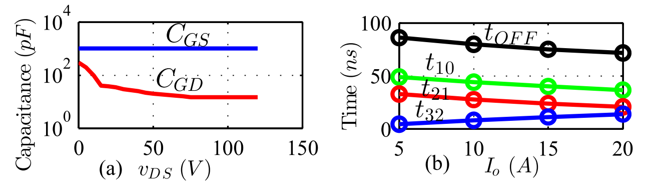

FIGURE 14. (a)Variation of C_{GD} and C_{GS} versus v_{DS}. (b) Plots of t_{10}, t_{21}, t_{32}, t_{OFF} versus current I_o from the analysis.

$$v_{GS} = V_{GG}e^{-(t-t_o)/(C_{GS}+C_{GD})R_G} \quad (2)$$

$$t_{10} = (t_1 - t_0) = R_G(C_{GS} + C_{GD})\ln\frac{g_m V_{GG}}{I_o + g_m V_{th}} \quad (3)$$

For $t_1 < t \leq t_2$, $v_{GS} = \frac{I_o}{g_m} + V_{th}$ and is constant and the necessary equations are shown further.

$$i_G = -C_{GD}\frac{dv_{DS}}{dt} = -\frac{(I_o/g_m) + V_{th}}{R_G} \quad (4)$$

$$dv_{DS} = \frac{(I_o/g_m) + V_{th}}{R_G C_{GD}}dt \quad (5)$$

Since C_{GD} is an unknown non-linear function of v_{DS}. Hence (5) is converted to difference equation and summed from $t = t_1$ to t_2 and $v_{DS} = 0$ to V_{DC}.

$$t_{21} = \sum_{i=1}^{n}\Delta t_i = \frac{R_G}{(I_o/g_m) + V_{th}}\sum_{i=1}^{n} C_{GD_i}\Delta v_{DS} \quad (6)$$

$$\text{For } t_2 < t \leq t_3,\ i_G = -\frac{v_{GS}}{R_G} = (C_{GS} + C_{GD})\frac{dv_{GS}}{dt} \quad (7)$$

Integrating (7) from $t = t_2$ to t_3, $v_{GS}(t_2) = (I_o/g_m) + V_{th}$ to $v_{GS}(t_3) = V_{th}$, and $t_3 - t_2$ is obtained.

$$t_{32} = (t_3 - t_2) = R_G(C_{GS} + C_{GD})\ln\left(1 + \frac{I_o}{V_{th}g_m}\right) \quad (8)$$

$$\text{Turn OFF time of MOSFET, } t_{OFF} = t_{10} + t_{21} + t_{32} \quad (9)$$

The variation of C_{GS} and C_{GD} with v_{DS} is shown in Fig. 14(a). Equation (3) is used to plot t_{10} against I_o. In this calculation, $C_{GD} = 300$ pF, $C_{GS} = 1035$ pF, $R_G = 20$ Ω including the internal gate resistance of 4.6 Ω of the MOSFET, $g_m = 8.1$ S, $V_{GG} = 20$ V, and $V_{th} = 2.6$ V. Further, (6) is used to plot t_{21}, where C_{GD} is non-linear. Therefore, sufficient number of values of C_{GD} is taken from the C_{GD} versus v_{DS} curve with $\Delta v_{DS} = 5$ V. The curve of t_{32} is traced using (8) where $C_{GD} = 15$ pF. Finally, the curve of t_{OFF} is traced using (9). The t_{OFF} plot shows a decreasing trend against increasing I_o, which matches the simulation trend of Fig. 12(b).

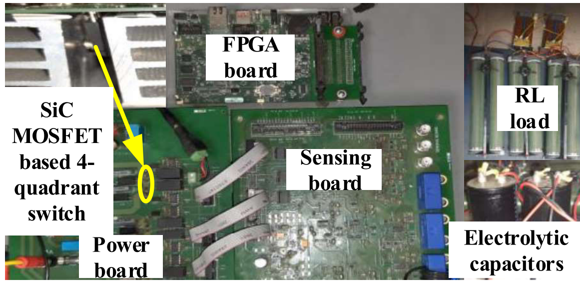

FIGURE 15. Test bench for the characteristics of 4-quadrant switch.

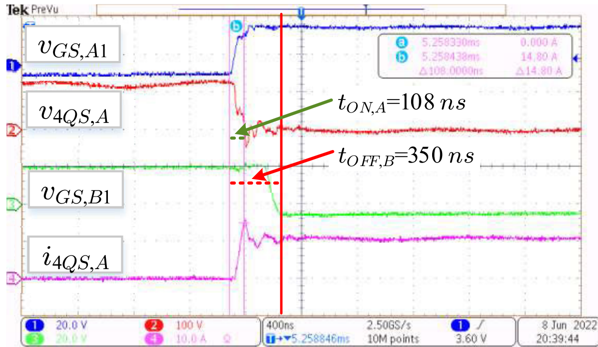

(a) First: turn ON; Fourth: turn OFF

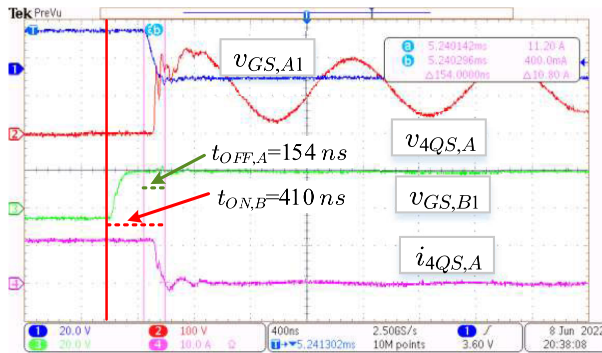

(b) First: turn OFF; Fourth: turn ON

FIGURE 16. Turn ON and OFF characteristics.

V. EXPERIMENTAL VERIFICATION

The test bench for finding the characteristics of the 4-quadrant switch is shown in Fig. 15. It consists of a power board, a sensing board, an FPGA board, a resistive load, an inductive load, and two electrolytic capacitors. The power board contains SiC MOSFETs connected in common-source configuration to create 4-quadrant switches. The voltage and current ratings of the SiC MOSFET are 1200 V and 36 A, respectively.

A. TURN ON/OFF TIME

This subsection presents the experimental results and trends for turn ON/OFF times in all four quadrants. Fig. 16 shows the turn ON of S_A in the first quadrant and the turn OFF of S_B in the fourth quadrant. The gate-source voltage, $v_{GS,A1}$, rises from -5 V to $+20$ V, $v_{4QS,A}$ falls from $+120$ V to $+5$ V and $i_{4QS,A}$ rises to $+15$ A in $t_{ON,A} = 108$ ns.

TABLE 1. Maximum turn ON/OFF time for 4-quadrant switch in all four quadrants.

Quadrant	Dominating devices	$t_{ON}(ns)$	$t_{OFF}(ns)$
First	S_{A1}	250	200
Second	S_{A2} and S_{B2}	420	350
Third	S_{A2}	250	200
Fourt	S_{A1} and S_{B1}	420	350

TABLE 2. Maximum turn ON/OFF time for 2-quadrant switch.

Quadrant	Dominating device	$t_{ON}(ns)$	$t_{OFF}(ns)$
First	S_A	250	200
Second	S_B	200	250

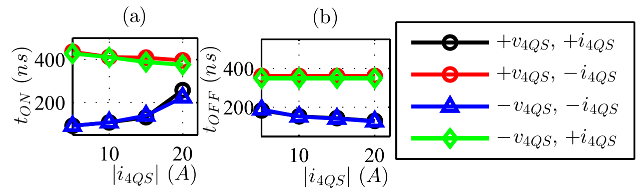

FIGURE 17. Plots of t_{ON} and t_{OFF} in all four quadrants. (a) t_{ON} versus $|i_{4QS}|$. (b) t_{OFF} versus $|i_{4QS}|$.

$v_{GS,B1}$ starts falling from $+20$ V towards -5 V after a delay of approximately 110 ns. The turn OFF time of S_B is, $t_{OFF,B} = 350$ ns. Fig. 16(b) presents the turn OFF of S_A in the first quadrant and turn ON of S_B in the fourth quadrant. The turn OFF time of S_A, $t_{OFF,A} = 154$ ns, and the turn ON time of S_B, $t_{ON,B} = 410$ ns. The intervals $t_{A1} = t_{A2} = t_{B1} = t_{B2} = 250$ ns.

The t_{ON} and t_{OFF} versus $|i_{4QS}|$ plots for all four quadrants obtained using the experiments are shown in Fig. 17(a) and Fig. 17(b), respectively. In first and third quadrants, t_{ON} increases from approximately 100 ns to 250 ns as $|i_{4QS}|$ increases from 5-20 A. Whereas, in the second and fourth quadrants, t_{ON} decreases from 420 ns to 380 ns as i_{4QS} increases from 5-20 A. t_{OFF} decreases from 200 ns to 100 ns against increasing $|i_{4QS}|$, for first and third quadrants. t_{OFF} in second and fourth quadrants are constant at 350 ns. The experimental trends exactly match with simulation trends though the values do not exactly match due to factors like unknown circuit parasitics and the approximate nature of LTSpice models. The reasons for these trends are already detailed in Section III.

Table 1 shows the dominating devices of each quadrant and the maximum turn ON/OFF time of the corresponding quadrant from the obtained experimental results. The maximum t_{ON} and t_{OFF} in the first and second quadrants are 250 ns and 200 ns, respectively. In the second and fourth quadrants, the maximum t_{ON} and t_{OFF} are 420 ns and 350 ns, respectively. The maximum t_{ON} and t_{OFF} of the 2-quadrant switch in the first quadrant are 250 ns and 200 ns, respectively, as shown in Table 2, are equal to 4-quadrant switch. But in second quadrant, the maximum t_{ON} of the 2-quadrant switch is 200 ns, which is 47% of the 4-quadrant switch. Also, t_{OFF} of the 2-quadrant switch is 250 ns and is 71% of the 4-quadrant switch. Therefore, a clear increase in t_{ON} and t_{OFF} are seen in the 4-quadrant switch compared 2-quadrant switch.

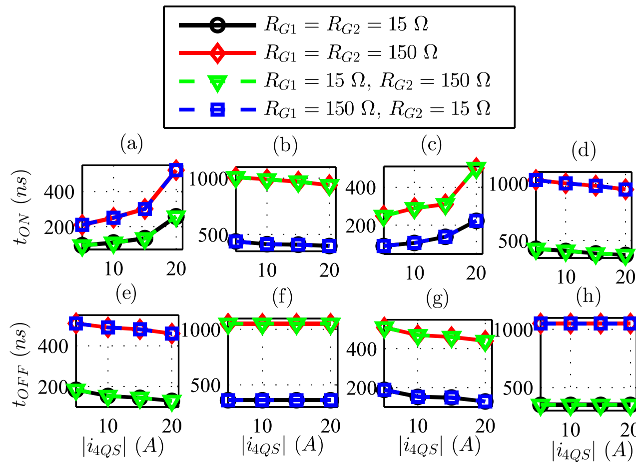

FIGURE 18. t_{ON} **versus** $|i_{4QS}|$**: (a) First (b) Second (c) Third (d) Fourth.** t_{OFF} **versus** $|i_{4QS}|$**: (e) First (f) Second (g) Third (h) Fourth.**

B. EFFECT OF GATE RESISTANCE

To show the effects of gate resistances on turn ON/OFF of the 4-quadrant switch, t_{ON} and t_{OFF} against $|i_{4QS}|$ are plotted for all quadrants in Fig. 18. The plots consider 15 and 150 Ω of gate resistances. Since the 4-quadrant switch has two SiC MOSFETs, so the gate resistances for both the MOSFETs are kept equal in the first case and in the second case, these resistances are unequal. The 4-quadrant switches S_A and S_B have simultaneous variations in gate resistances with similar values so that both switches remain identical. The turn ON and turn OFF plots for all the conditions are explained further.

1) ON TURN ON

The graphs in Fig. 18(a)-(d) show the effect of gate resistances on t_{ON} of S_A. Fig. 18(a) shows the plots in the first quadrant. t_{ON} increases as the gate resistances increase. The current direction is positive in this case; therefore, R_{G1} of S_A decides t_{ON}, as discussed in Section II, which is evident from the graphs. The graphs in Fig. 18(b) suggest that t_{ON} increases with an increase in gate resistance in second quadrant. In this condition, the current direction is opposite, and hence R_{G2} of both S_A and S_B decide t_{ON}. Further, Fig. 18(c) represents plots for third quadrant and t_{ON} increases as the gate resistances increase, and since the current is negative so R_{G2} of only S_A decides t_{ON}. The graphs in Fig. 18(d) for fourth quadrant also convey similar trends of increasing t_{ON} and R_{G1} of both S_A and S_B determine t_{ON}.

2) ON TURN OFF

The graphs in Fig. 18(e)-(h) show the effect of gate resistances on t_{OFF}. Fig. 18(e) shows the plots in first quadrant. t_{OFF} increases as the gate resistance increases. The current direction is positive; therefore, the gate resistance R_{G1} of S_A determines t_{OFF}. The graphs in Fig. 18(f) suggest that t_{OFF} increases with an increase in gate resistance in second quadrant. In this condition, the current direction is opposite, and hence R_{G2} of S_A and S_B both decide t_{OFF}. Further, Fig. 18(g) represents plots in third quadrant and t_{OFF} increases with an increase in gate resistance. Since current is negative so R_{G2} of S_A determines t_{OFF}. The graphs in Fig. 18(h) show trends of increasing t_{OFF} with increasing R_{G1} of S_A and S_B both.

C. OVERALL INFERENCES

The overall inferences from this section are:

- The turn ON time is smaller in first and third quadrants than in second and fourth quadrants. Also, in first and third quadrants, the turn ON time is similar and increases with the current. In comparison, the turn ON time in second and fourth quadrants is similar but decreases with the current owing to the turn OFF time of the complementary 4-quadrant switch.
- The turn OFF time is lower in first and third quadrants than in second and fourth quadrants. It decreases with an increase in current in first and third quadrants, whereas it remains constant with an increase in current in second and fourth quadrants. The reasons have been discussed in Section IV.
- The comparison of the maximum turn ON/OFF time of the 4-quadrant switch and 2-quadrant suggests that the switching frequency of the 4-quadrant switch gets reduced due to higher turn ON/OFF time in second quadrant operation.
- The increase in gate resistance increases the turn ON/OFF time in all quadrants. In first and third quadrants, only the gate resistance of the MOSFET carrying positive current influences the turn ON/OFF time. But in second and fourth quadrants, the gate resistances of the MOSFETs carrying a positive current of both the 4-quadrant switches affect the turn ON/OFF time. Hence it verifies the dominating devices for turn ON/OFF time in each quadrant.

VI. CONCLUSION

This paper performs a detailed analytical, simulation, and experimental investigation on the turn ON/OFF time of SiC MOSFET based 4-quadrant switch in all four quadrants. The investigation shows that only one device affects the turn ON/OFF time in first and third quadrants and two devices affect the turn ON/OFF time in second and fourth quadrants. The turn ON time is lesser in first and third quadrants than in second and fourth quadrants. Also, with an increase in current, turn ON time increases in first and third quadrants, whereas it decreases in second and fourth quadrants. The turn OFF time decreases in first and third quadrants and remains constant in second and fourth quadrants. The switching frequency of the 4-quadrant switch is higher than the 2-quadrant switch as the maximum turn ON/OFF time is higher in second quadrant for the 4-quadrant switch. The experimental results with unequal gate resistances for the 4-quadrant switch verify the dominating devices of the respective quadrants. Hence, the gate resistances of the dominating devices determine the turn ON/OFF time. Also, the increase in the gate resistances of the dominating devices increases the turn ON/OFF time.

REFERENCES

[1] H. Chen and D. Divan, "High speed switching issues of high power rated silicon-carbide devices and the mitigation methods," in *Proc. IEEE Energy Convers. Congr. Expo. (ECCE)*, Sep. 2015, pp. 2254–2260.

[2] S. Hazra, A. De, L. Cheng, J. Palmour, M. Schupbach, B. A. Hull, S. Allen, and S. Bhattacharya, "High switching performance of 1700-V, 50-A SiC power MOSFET over Si IGBT/BiMOSFET for advanced power conversion applications," *IEEE Trans. Power Electron.*, vol. 31, no. 7, pp. 4742–4754, Jul. 2016.

[3] S. Ji, S. Zheng, F. Wang, and L. M. Tolbert, "Temperature-dependent characterization, modeling, and switching speed-limitation analysis of third-generation 10-kV SiC MOSFET," *IEEE Trans. Power Electron.*, vol. 33, no. 5, pp. 4317–4327, May 2018.

[4] M. Imaizumi and N. Miura, "Characteristics of 600, 1200, and 3300 V planar SiC-MOSFETs for energy conversion applications," *IEEE Trans. Electron Devices*, vol. 62, no. 2, pp. 390–395, Feb. 2015.

[5] S. Jahdi, O. Alatise, P. Alexakis, L. Ran, and P. Mawby, "The impact of temperature and switching rate on the dynamic characteristics of silicon carbide Schottky barrier diodes and MOSFETs," *IEEE Trans. Ind. Electron.*, vol. 62, no. 1, pp. 163–171, Jan. 2015.

[6] M. Nymand and M. A. E. Andersen, "High-efficiency isolated boost DC–DC converter for high-power low-voltage fuel-cell applications," *IEEE Trans. Ind. Electron.*, vol. 57, no. 2, pp. 505–514, Feb. 2010.

[7] H. Zhang and L. M. Tolbert, "Efficiency impact of silicon carbide power electronics for modern wind turbine full scale frequency converter," *IEEE Trans. Ind. Electron.*, vol. 58, no. 1, pp. 21–28, Jan. 2011.

[8] B. Whitaker, A. Barkley, Z. Cole, B. Passmore, D. Martin, T. R. McNutt, A. B. Lostetter, J. S. Lee, and K. Shiozaki, "A high-density, high-efficiency, isolated on-board vehicle battery charger utilizing silicon carbide power devices," *IEEE Trans. Power Electron.*, vol. 29, no. 5, pp. 2606–2617, May 2014.

[9] K. Koiwa and J.-I. Itoh, "A maximum power density design method for nine switches matrix converter using SiC-MOSFET," *IEEE Trans. Power Electron.*, vol. 31, no. 2, pp. 1189–1202, Feb. 2016.

[10] J. A. Cooper and A. Agarwal, "SiC power-switching devices-the second electronics revolution?" *Proc. IEEE*, vol. 90, no. 6, pp. 956–968, Jun. 2002.

[11] S. Safari, A. Castellazzi, and P. Wheeler, "Experimental and analytical performance evaluation of SiC power devices in the matrix converter," *IEEE Trans. Power Electron.*, vol. 29, no. 5, pp. 2584–2596, May 2014.

[12] P. W. Wheeler, J. Rodriguez, J. C. Clare, L. Empringham, and A. Weinstein, "Matrix converters: A technology review," *IEEE Trans. Ind. Electron.*, vol. 49, no. 2, pp. 276–288, Apr. 2002.

[13] U. Raheja, G. Gohil, K. Han, S. Acharya, B. J. Baliga, S. Battacharya, M. Labreque, P. Smith, and R. Lal, "Applications and characterization of four quadrant GaN switch," in *Proc. IEEE Energy Convers. Congr. Expo. (ECCE)*, Oct. 2017, pp. 1967–1975.

[14] W. Song, W. Zhang, B. Ren, and Y. Zhong, "Bidirectional switching characteristics analysis based on SiC MOSFET," in *Proc. Chin. Autom. Congr. (CAC)*, Nov. 2018, pp. 2949–2954.

[15] M. Baus, B. N. Szafranek, S. Chmielus, M. C. Lemme, B. Hadam, B. Spangenberg, R. Sittig, and H. Kurz, "Fabrication of monolithic bidirectional switch (MBS) devices with MOS-controlled emitter structures," in *Proc. IEEE Int. Symp. Power Semiconductor Devices*, Jun. 2006, pp. 1–4.

[16] S. Chowdhury, C. W. Hitchcock, Z. Stum, R. P. Dahal, I. B. Bhat, and T. P. Chow, "Operating principles, design considerations, and experimental characteristics of high-voltage 4H-SiC bidirectional IGBTs," *IEEE Trans. Electron Devices*, vol. 64, no. 3, pp. 888–896, Mar. 2017.

[17] M. J. Bland, P. W. Wheeler, J. C. Clare, and L. Empringham, "Comparison of Bi-directional switch components for direct AC–AC converters," in *Proc. IEEE 35th Annu. Power Electron. Spec. Conf.*, vol. 4, Jun. 2004, pp. 2905–2909.

[18] S. Mori, M. Aketa, T. Sakaguchi, Y. Nanen, H. Asahara, T. Nakamura, and T. Kimoto, "High-temperature characteristics of 3-kV 4H-SiC reverse blocking MOSFET for high-performance bidirectional switch," *IEEE Trans. Electron Devices*, vol. 64, no. 10, pp. 4167–4174, Oct. 2017.

[19] L. Wang, X. Zhang, J. Deng, J. Yang, O. K. Oladele, and Y. Zhao, "Unwanted turn-on of SiC JFET Bi-directional switches under influence of parasitic parameters," in *Proc. 43rd Annu. Conf. IEEE Ind. Electron. Soc. (IECON)*, Oct. 2017, pp. 4194–4199.

[20] H. Dai, R. A. Torres, T. M. Jahns, and B. Sarlioglu, "Characterization and implementation of hybrid reverse-voltage-blocking and bidirectional switches using WBG devices in emerging motor drive applications," in *Proc. IEEE Appl. Power Electron. Conf. Expo. (APEC)*, Mar. 2019, pp. 297–304.

[21] B. Fan, V. Baker, R. Burgos, M. E. Chamie, W. Chen, V. Blasko, and D. Boroyevich, "Common-source inductance induced voltage overshoot and oscillation in active bidirectional devices," *IEEE Trans. Power Electron.*, vol. 36, no. 12, pp. 13383–13388, Dec. 2021.

[22] N. Anurag and S. Nath, "Effect of commutation control on switching frequency of SiC based four quadrant switch," in *Proc. Nat. Power Electron. Conf. (NPEC)*, Dec. 2021, pp. 1–6.

[23] M. Rashid, *Power Electronics Handbook*, 3rd ed. London, U.K.: Academic Press, 2011, ch. 4, pp. 43–71.

NISHANT ANURAG (Graduate Student Member, IEEE) received the B.Tech. degree from the Kalinga Institute of Industrial Technology, Bhubaneswar, Odisha, India, in 2013. He is currently pursuing the joint M.S. and Ph.D. degrees in power engineering with the Department of Electronics and Electrical Engineering, IIT Guwahati, Assam, India.

From 2014 to 2015, he was a Software Engineer at Aricent, Gurgaon, Haryana, India. His research interests include the SiC MOSFET-based bidirectional switch, matrix converter, and solid-state transformer.

SHABARI NATH (Member, IEEE) received the B.E. degree from Rajiv Gandhi Proudyogiki Vishwavidyalaya, Bhopal, India, in 2005, the M.Tech. degree from IIT Bombay, Mumbai, India, in 2008, and the Ph.D. degree from the University of Minnesota, Minneapolis, MN, USA, in 2012, all in electrical engineering.

She was a Product Design Engineer at Cummins Inc., Columbus, IN, USA, for two years. Since 2014, she has been an Associate Professor with the Department of Electronics and Electrical Engineering, IIT Guwahati, India. Her research interests include multiport converters, solid-state transformers, power electronic converters for renewable energy systems, and smart microgrids.